Available online at www.sciencedirect.com
ScienceDirect
Journal of Power Sources 161 (2006) 1385–1391
JOURNAL OF POWER SOURCES
www.elsevier.com/locate/jpowsour

The effect of the charging protocol on the cycle life of a Li-ion battery

Sheng Shui Zhang *

U.S. Army Research Laboratory, AMSRD-ARL-SE-DC, Adelphi, MD 20783-1197, USA

Received 16 April 2006; received in revised form 22 May 2006; accepted 6 June 2006
Available online 28 July 2006

Abstract

The effect of the charging protocol on the cycle life of a commercial 18650 Li-ion cell was studied using three methods: (1) constant current (CC) charging, (2) constant power (CP) charging, and (3) multistage constant current (MCC) charging. The MCC-charging consists of two CC steps, which starts with a low current to charge the initial 10% capacity followed by a high current charging until the cell voltage reaches 4.2 V. Using these methods, respectively, the cell was charged to 4.2 V followed by a constant voltage (CV) charging until the current declined to 0.05 C. Results showed that the cycle life of the cell strongly depended on the charging protocol even if the same charging rate was used. Among these three methods, the CC-method was found to be more suitable for slow charging (0.5 C) while the CP-method was better for fast charging (1 C). Impedance analyses indicated that the capacity loss during cycling was mainly attributed to the increase of charge-transfer resistance as a result of the progressive growth of surface layers on the surface of two electrodes. Fast charging resulted in an accelerated capacity fading due to the loss of Li^+ ions and the related growth of a surface layer, which was associated with metallic lithium plating onto the anode and a high polarization at the electrolyte–electrode interface. Analyses of the cell electrochemistry showed that use of a reduced current to charge the initial 10% capacity and near the end of charge, respectively, was favorable for long cycle life.
Published by Elsevier B.V.

Keywords: Li-ion battery; 18650 cell; Charging; Cycle life; Impedance

1. Introduction

Li-ion batteries have been extensively used in many portable electronic devices such as laptop computers, camcorders and cellular phones. Most of these batteries in the current market employ a graphite-based anode, into which Li^+ ions are able to intercalate and de-intercalate in a narrow potential range of 0.05–0.3 V versus Li^+/Li through multistage phase transitions [1,2]. In particular, the potential of the last phase transition from LiC_{12} to LiC_6 is known to be as low as 0.065 V versus Li^+/Li. This implies that the maximum over-potential for the graphite anode during charging a Li-ion battery cannot exceed 0.065 V. Otherwise, metallic lithium plating inevitably occurs on the anode, which not only destroys solid electrolyte interface (SEI) on the surface of graphite and reduces cycling efficiency, but also raises safety concerns due to the internal short circuiting caused by the formation of dendritic lithium. In order to alleviate the unwanted lithium plating, Li-ion batteries are required to be charged through two continuous steps. That is, the battery is charged at a constant current until its voltage reaches the pre-determined limit (4.1 or 4.2 V) followed by a constant voltage charging until the current declines to a pre-determined low value. This method is called constant current–constant voltage (CC–CV) charging. In our recent work [3], however, we found that metallic lithium plating can occur near the end of CC-charging step during a normal CC–CV charging as long as the charging current rate reaches or exceeds a certain value. In such cases further increasing of the current rate does not shorten the total charging time significantly, instead it greatly increases the CV-charging time and the battery chemistry deteriorates as a result of the unwanted reactions between the plated metallic lithium and the electrolyte components. Therefore, searching for an appropriate charging protocol is essential for Li-ion batteries to achieve a balance between a short charging time and a long cycle life.

In addition to using electrode active materials with small particle sizes and modifying the cell design (such as by reducing the electrode loading/thickness and increasing the content of

* Tel.: +1 301 394 0981; fax: +1 301 394 0273.
E-mail address: szhang@arl.army.mil.

0378-7753/$ – see front matter. Published by Elsevier B.V.
doi:10.1016/j.jpowsour.2006.06.040

conducting carbon), several efforts have been devoted to study the charging techniques and charging protocols. The techniques that have been reported for fast charging or healthy charging include boost charging [4], multistage CC-charging [5,6], current decay charging [7–9], and dynamic pulse charging [10–13]. Regardless of the charging techniques, a short charging time is achieved always at the expense of cycle life with few exceptions [13]. There must be an optimized charging protocol that can balance fast charging and healthy cycling for the Li-ion batteries. In this work, two other charging protocols were designed to compare the conventional CC–CV method. The correlation between charging protocol and cycle life of the Li-ion batteries was studied and discussed by using these three methods with the same charging rate.

2. Experimental

Two charging protocols, constant power–constant voltage (CP–CV) and multistage constant current–constant voltage (MCC–CV), were designed to study the effect of the charging protocol on cycle life of the Li-ion cells by comparing them with conventional CC–CV charging. In all protocols, a CV-charging was applied to achieve the fully charged state after the cell voltage reached 4.2 V until the current declined to 0.05 C. The CP-charging features a current that starts with a high value and gradually decreases with the charging time following a correlation of constant power until the voltage reaches to 4.2 V. The MCC-charging consists of two CC steps, which starts with a low CC-charging for a certain time, followed by a high CC-charging until the voltage reaches 4.2 V (more details will be described in Section 3). For a fair comparison, the same charging rate (time) was used in the three protocols. The charging rate for the CC- and MCC-charging, respectively, was determined from the initial capacity (Ah), whereas that for the CP-charging was calculated from the initial charging energy (Wh). In all cycling tests, the cell was CC-discharged to 2.5 V at the same rate as used in charging.

Commercial $LiCoO_2$-based 18650 cells were used as the test vehicles. Manufacturer product data sheet shows that these types of cells have an average weight of 47 g and a rated capacity of 2.4 Ah between 2.5 and 4.2 V. Since the cells had been stored for more than 3 years before test, their initial capacity and energy were determined by charging and discharging for three cycles using a 1.2 A CC–CV protocol. Three cells were used for each charging protocol and the one with middle performance was selected for discussion. In an increment of every 100 cycles, the cycling test was interrupted and the cell was brought to the fully charged state using a 0.5 C CC–CV protocol, followed by impedance measurement. In order to monitor the potential change of the cathode and graphite anode in the various charging protocols, a three-electrode electrochemical cell with metallic lithium foil as the reference electrode was assembled and cycled using three independent channels, of which one channel was used to cycle the cell and the other two channels were used to record the potential of the cathode and anode, respectively. The detailed procedure and connection circuitry are described in our earlier paper [3]. In this cell, the electrode loading was 2.56 mAh cm^{-2} for the graphite anode and 2.36 mAh cm^{-2} for the $LiCoO_2$ cathode, respectively, and the electrolyte was a solution of 1.2 M $LiPF_6$ dissolved in a 3:7 (wt.) mixed solvent of ethylene carbonate (EC) and ethyl methyl carbonate (EMC). Before the test, the cell was formed by charging and discharging at 0.1 C for two cycles, followed by cycling at 0.5 C between 2.5 and 4.2 V for five times using a CC–CV charging protocol with an ending current limit of 0.05 C.

A Maccor Series 4000 tester was employed for cycling tests. A Solartron SI 1287 Electrochemical Interface and SI 1260 Impedance/Gain-Phase Analyzer were used for the impedance measurements, which were performed over a frequency range from 100 kHz to 0.01 Hz using a 5 mV AC oscillation. For the measurements at various states, the cell was discharged at 0.05 C for a certain time and then rested for 1 h to reach a stable open-circuit voltage (OCV), followed by impedance measurement. This procedure was started from the fully charged state and progressively repeated until the cell was discharged to 2.5 V. The resulting AC impedance spectra were analyzed using Zview software (Scribner and Associates, Inc.). All measurements were carried out at room temperature (about 23 °C). For description, the ratio of discharging capacity at a specific state to that obtained by discharging at 0.5–2.5 V was defined as the state-of-charge (SOC).

3. Results and discussion

3.1. Characteristics of the charging protocols

Three charging protocols with the same charging rate were, respectively, used to charge the Li-ion cells until the voltage reached 4.2 V followed by CV-charging until the current declined to 0.05 C. Fig. 1 shows the characteristics of these protocols having an averaged charging rate of 0.5 C. A common characteristic is that with each protocol the cell could be charged to 0.82–0.84 SOC at the point where the voltage reached 4.2 V and that the rest SOC was a top-up by the subsequent CV-charging. CC-charging shows that the SOC is linearly increased with the charging time until the voltage reached 4.2 V followed by a slow increase due to a decrease of the current in the following CV-charging. In CP-charging, the current starts with a relatively high value and it gradually decreases with charging time, during which there always exists a CP-correlation between the current and voltage. After the voltage reaches 4.2 V, CV-charging is followed until the current declined to the pre-determined value (0.05 C).

For the MCC-protocol, there are many combinations between the current and charging time for two CC-charging steps to meet the pre-determined *C*-rate. To simplify, we applied an additional condition to this protocol. That is, the initial 10% capacity was charged using half of the pre-determined *C*-rate, followed by charging at an increased *C*-rate until the voltage reached 4.2 V. Based on this condition, the current rate and charging time for various averaged *C*-rates can be calculated and summarized in Table 1, in which the conditions shown in the last two columns were used in this work.

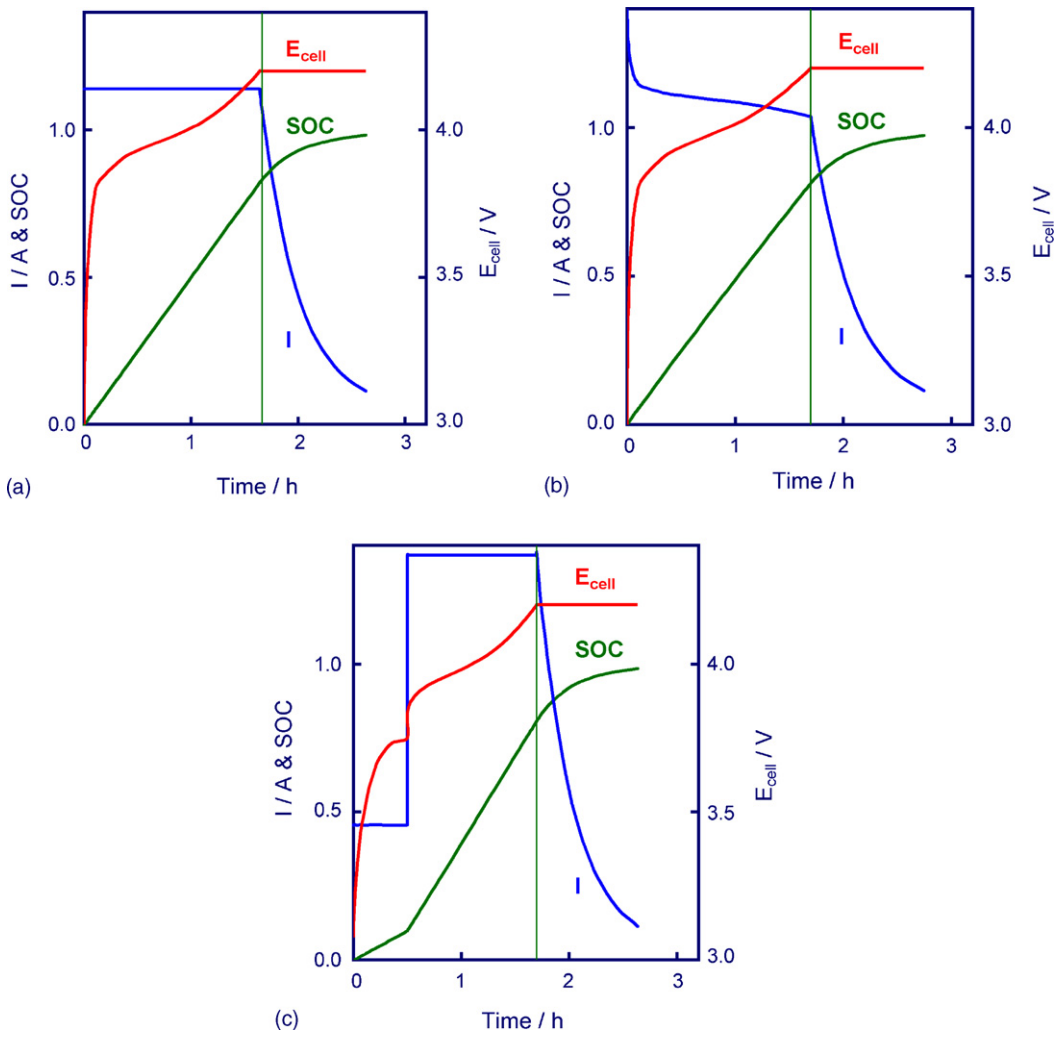

Fig. 1. Characteristics of the charging protocols for a commercial 2.4 Ah 18650 Li-ion cell using an averaged charging rate of 0.5 C: (a) CC–CV, (b) CP–CV, and (c) MCC–CV. Note that the MCC shows a procedure charging at 0.2 C for 0.5 h followed by charging at 0.57 C until the voltage reaches 4.2 V.

3.2. Impact of the charging protocol on cycle life

Fig. 2 compares cycling performances of Li-ion cells using three charging protocols, in which the cells were cycled at 0.5 C for 100 cycles, followed by charging and discharging at 1 C for the rest of test. It is shown that initially three cells have a very similar capacity of ~2.3 Ah, but the capacity fades with cycle number in different ways. Obviously, the cycling rate and charging protocol strongly affect the rate of capacity fading. At a low cycling rate (0.5 C), the rate of capacity fading increases in the order of CP > MCC > CC, while it turns to the order of MCC > CC > CP when the cycling rate is increased to 1 C.

Fig. 3 shows the correlation of the discharging capacity, CV-charging capacity and portion of CV-capacity with cycle number for the CC–CV protocol, in which the portion of CV-capacity is defined as the ratio of the CV-charging capacity to the sum of CC- and CV-charging capacities and is generally an indication of the effectiveness of a charging protocol. For a given cell system, the value of the portion of CV-capacity reflects a charging rate while an increase in the value corresponds to a loss in the capacity and power. For long cycle life, the portion of CV-

Table 1
C-rate and time used in MCC-charging protocol with an averaged *C*-rate

CC-charging step number	*C*-rate[a]	Time	$N = 0.5$ C	$N = 1$ C
Averaged *C*-rate	N	$1/N$	0.5 C for 2 h	1 C for 1 h
1. Charging at half of *C*-rate to 10% capacity	$0.5N$	$0.2/N$	0.25 C for 0.4 h	0.5 C for 0.2 h
2. Charging at high rate until voltage reaches 4.2 V	$1.125N$	$0.8/N$	0.5625 C for 1.6 h	1.125 C for 0.8 h

Right two columns are the conditions used in this work.
[a] N is the averaged *C*-rate that was pre-determined for a given MCC–CV protocol.

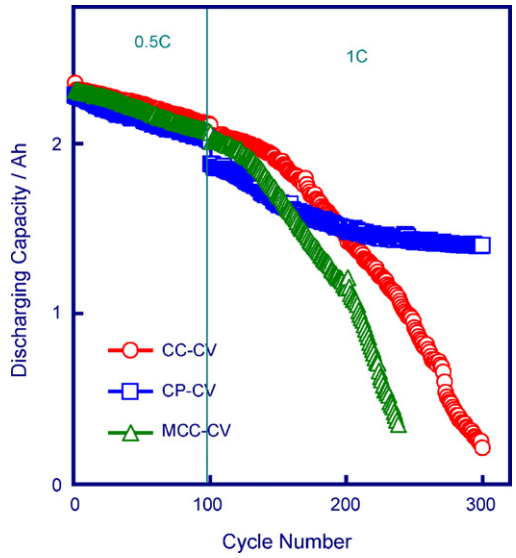

Fig. 2. Cycling performance of Li-ion cells by different charging protocols, in which the cell was charged and discharged at 0.5 C for the first 100 cycles and then at 1 C for the rest of cycles.

capacity should be designed not to exceed 0.3. Otherwise, the cell suffers an accelerated capacity fading due to high polarization caused by the local imbalance between the cell reaction and ionic diffusion on the electrolyte–electrode interface and resulting metallic lithium plating on the anode or overcharge on the cathode, which depends on the ratio of the reversible capacity of the cathode to the anode [3]. As shown in Fig. 3, the portion of CV-capacity at 0.5 C is 0.16 in the beginning of cycling, and it slowly increases with cycle number. When the cycling rate was increased to 1 C, the portion of CV-capacity immediately jumped to higher than 0.5. As a result, it promoted fading of the discharging capacity with progressive cycling. In particular, the CV-capacity was decreased with cycle number starting from about the 180th cycle and finally approached discharging capacity after 250 cycles. In the latter case, most of the capacities are charged through CV-charging, instead of CC-charging. These phenomena are mostly accompanied by significantly fast capacity fading and are believed to be associated with the decrease of charging efficiency probably due to metallic lithium plating onto the graphite anode and its resulting reactions with the electrolyte components. The facts above reveal that 1*C*-rate might not be suitable for the present Li-ion cell.

Fig. 4 exhibits the effect of the charging protocol on the CV-capacity. It is clear that increasing rate of the portion of CV-capacity is dependent on charging protocol and charging rate. Comparing with Fig. 2, one may find a mirror-like correlation in the change of discharging capacity and CV-capacity with cycle number. More interestingly, the increase of CV-capacity is mostly in parallel with the growth of cell internal impedance. Therefore, one may plot the portion of the CV-capacity versus cycle number as an easy and convenient method to evaluate a charging protocol or to diagnose an aging of cell chemistry.

3.3. AC impedance analysis

Fig. 5 shows a typical impedance spectrum of an 18650 cell, which starts with an inductive tail at very high frequency (>1000 Hz) followed by two over-lapped semicircles through high to middle frequency and a straight line at low frequency. The inductive tail at very high frequency is changed with the cell design and electrode structure, and in the case of 18650 cells it could be attributed to the jelly-roll configuration and porous electrode structure [13,14]. Therefore, only the parts above real axis can be used to expect cell life. The intersection of the diagram with real axis refers to a bulk resistance (R_b), which reflects the sum of ohmic resistances of the electrolyte and of the other resistive components such as separator, current collectors, and cell connectors. The semicircle at high frequency reflects resistance (R_{sei}) and capacitance (C_{sei}) of the solid electrolyte interface or called surface layer on the surface of two electrodes. Since both R_b and R_{sei} are of pure ohmic characteristic, we called their sum as ohmic resistance (R_{ohm}). The semicircle at middle fre-

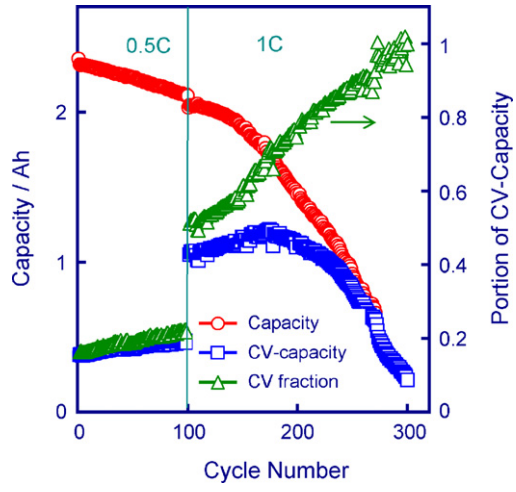

Fig. 3. Discharging capacity, CV-charging capacity and portion of CV-charging capacity as a function of cycle number for a Li-ion cell using CC–CV protocol.

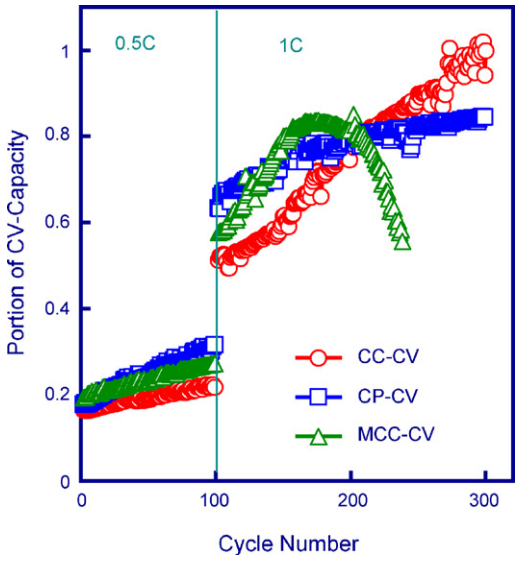

Fig. 4. Increase of the portion of CV-charging capacity with cycle number by different charging protocols.

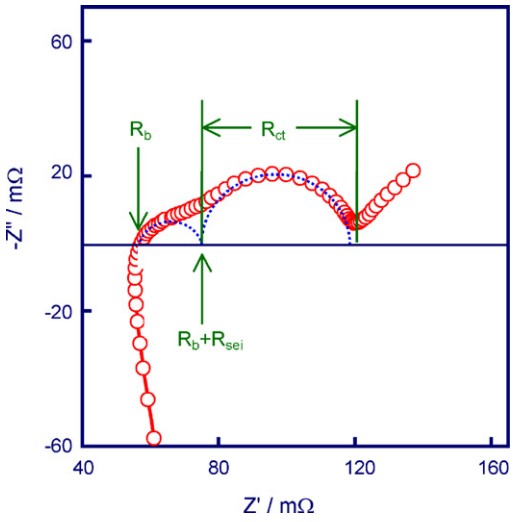

Fig. 5. Impedance spectroscopy of an 18650 Li-ion cell.

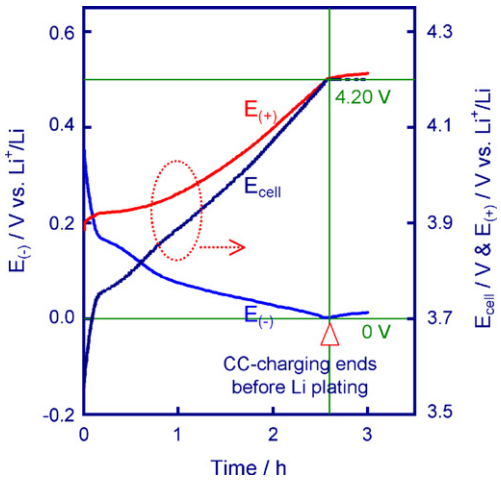

Fig. 7. An optimized CC–CV charging protocol recorded from a three-electrochemical Li-ion cell at 0.33 C.

quency and its following straight line are responded to Faradic processes, which reflect charge-transfer impedance and Warburg impedance. The charge-transfer impedance is attributed to charge-transfer resistance (R_{ct}) and its related double-layer capacitance (C_{dl}). Warburg impedance is related to diffusion of Li^+ ions on the interface between the active material particles and electrolyte.

Since R_{ct} of Li-ion cell is strongly SOC-dependent, the cells with the same SOC should be used for the purpose of impedance analysis. In this work, the fully charged state was selected to evaluate the effect of charging protocols on the cycle life. Fig. 6a and b compares R_{ohm} and R_{ct}, respectively, of the cells cycled by different charging protocols. A general trend is that both R_{ohm} and R_{ct} grow with cycle number regardless of the charging protocols. Comparing Fig. 6a and b, one finds that (1) growth rate of both R_{ohm} and R_{ct} increases with the charging rate, (2) R_{ct} grows much faster than R_{ohm}, and (3) there is no distinct correlation between cell impedance and cell capacity (by comparing Figs. 6 and 2). It is known that the growth of R_{ohm} is mainly attributed to the progressive growth of the surface layers and its related consumption of electrolyte, while that of R_{ct} is attributed to the deterioration of cell reaction kinetics. A good charging protocol should reflect cell chemistry to minimize the growth of R_{ct}.

3.4. Charging protocol versus cell electrochemistry

As mentioned above, there is no clear correlation between capacity and impedance. To understand this observation, we examined potentials of the cathode and anode using a three-electrode cell. Fig. 7 shows the change of cell voltage, cathode potential and anode potential with charging time by an optimized CC–CV protocol. For healthy charging, the potentials of cathode and anode should be strictly remained within the limiting values, as shown by two horizontal straight lines in Fig. 7. Beyond these limiting values, the cathode would be overcharged and meanwhile the high potential could result in oxidization of electrolytic solvents. By contrast, metallic lithium plating could

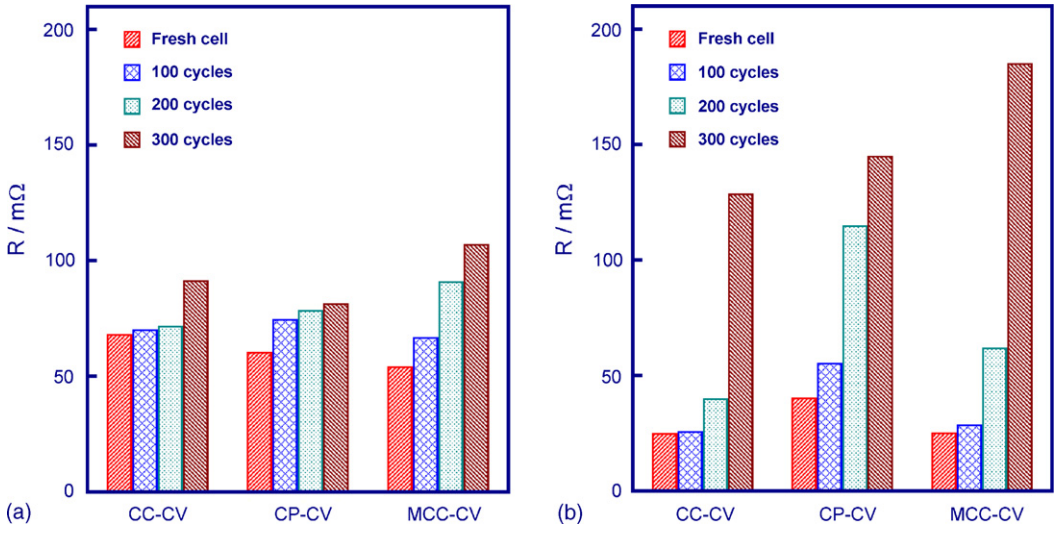

Fig. 6. Comparison of the ohmic resistance (a) and charge-transfer resistance (b) for 18650 cells by different charging protocols.

occur on the anode. Although the plated lithium can intercalate into graphite, its efficiency must be reduced due to the unwanted reactions between the plated metallic lithium and electrolytic solvents. As shown in Fig. 7, the CC-charging ends just before the potential of graphite decreases to 0 V versus Li^+/Li, and the potential slowly goes up in the following CV-charging due to a decrease in the current. Therefore, the charging protocol in Fig. 7 is an optimized one that achieves a good balance between fast charging and healthy cycling.

Fig. 8 shows electrochemical characteristics of a MCC–CV protocol using an averaged rate of 0.5 and 1 C, respectively. This protocol was designed to reduce the initial polarization by charging the initial 10% capacity at a reduced current rate (to be discussed later). Due to the use of rather high current rate in the second CC step, the potential of graphite falls to below 0 V versus Li^+/Li before the end of CC-charging. As a result, metallic lithium plating takes place between the surface and SEI of graphite particles, which inevitably destructs the existing SEI. In addition to re-intercalating into graphite, the plated lithium having very high surface area will react with electrolytic solvents, which consequently promotes progressive growth of the SEI. Furthermore, the potential of graphite is unable to rise above 0 V versus Li^+/Li in the end of CV-charging due to the electric polarization caused by the pre-determined limiting current. In such cases the cathode during CV-charging has lower potential than the Li-ion cell (see Fig. 8a and b), suggesting that capacity of the cathode cannot be fully utilized. The above analyses indicate that the MCC–CV charging protocol is neither effective nor healthy for Li-ion cell.

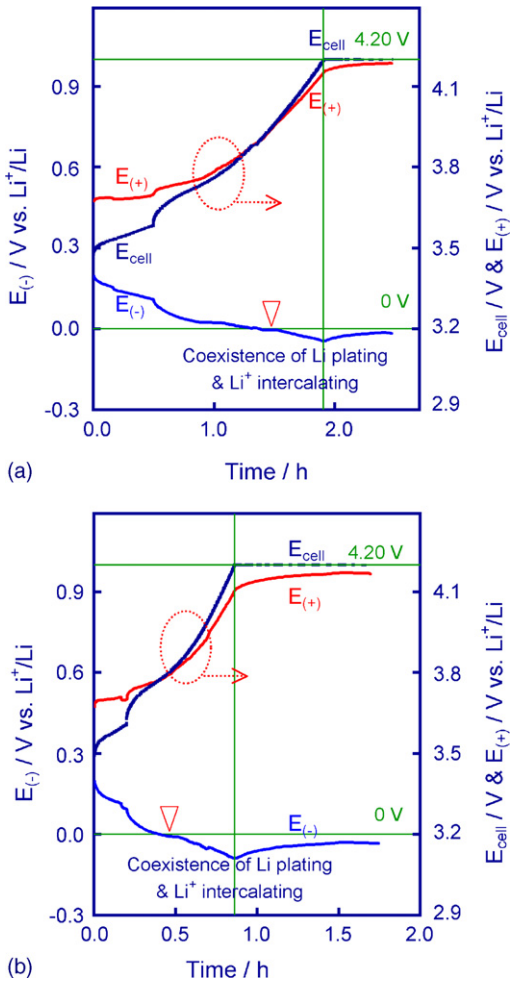

Fig. 8. Correlation of the cell voltage and electrode potentials for a three-electrode Li-ion cell using a MCC–CV charging protocol at: 0.5 C (a) and 1 C (b), respectively.

The CP–CV protocol was designed to solve the problem of metallic lithium plating near the end of charging. This method features the current gradually decreasing with the charging time (see Fig. 1b). Surprisingly, it results in faster capacity fading when the charging rate is low (0.5 C, Fig. 2). To understand this abnormal phenomenon, we plotted cell resistance (R_{cell}), R_{ohm}, and R_{ct} versus SOC of the cell in Fig. 9. It is shown that with respect to SOC of the cell, the R_{ohm} changes very little, while the R_{ct} changes dramatically. With the SOC decreasing to 0.1, the R_{ct} is sharply increased, which results in a sharp increase in the R_{cell}. This characteristic is the main reason why a low current was selected to charge the initial 10% capacity in the MCC–CV charging protocol. Therefore, the fast capacity fading observed from 0.5 C CP–CV charging could be attributed to the initial high polarization caused by these two factors of: (1) the initial high current applied in the CP-charging, and (2) the extremely high R_{cell} determined by the cell chemistry. It should be noted that the advantage of the CP–CV protocol becomes apparent when the charging rate is increased to 1 C (Fig. 2). This can be attributed to its lower current near the end of CP-charging, which favors reducing metallic lithium plating.

The discussion above suggests that a healthy charging protocol for Li-ion chemistry should use relatively low currents in the beginning and near the end of charging. The low current in the beginning (i.e., the initial 10% capacity) is used to compensate for high cell impedance, whereas the low current near the end is applied to alleviate metallic lithium plating.

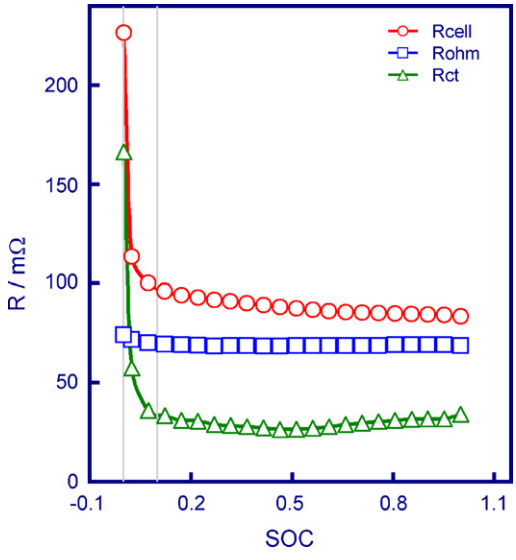

Fig. 9. Cell resistance (R_{cell}), ohmic resistance (R_{ohm}), and charge-transfer resistance (R_{ct}) as a function of the state-of-charge (SOC), which was recorded from an 18650 Li-ion cell at 20 °C.

4. Conclusions

From the results of this work, it may be concluded that cycle life of Li-ion cells is significantly affected by the charging protocol even if the same charging rate is applied. A good charging protocol should strictly follow the cell chemistry. Impedance analysis shows that the cell with a low SOC (<0.1) has a much higher resistance, which suggests that a low charging rate be desirable for charging the initial 10% capacity. Potential monitoring indicates that due to electric polarization, the potential of the graphite anode may fall to below 0 V versus Li^+/Li near the end of charging so that metallic lithium plating can occur on the anode. Although the plated metallic lithium can continue to intercalate into the graphite, it inevitably reacts with the electrolyte solvents, which not only reduce charging efficiency but also promote progressive growth of the resistive surface layer. Therefore, a low charging rate is favorable for healthy charging near the end of charging. It is shown that the capacity loss of a Li-ion cell during cycling is associated with increased cell impedance and reduced charging efficiency relating to metallic lithium plating on the anode.

References

[1] J.R. Dahn, R. Fong, M.J. Spoon, Phys. Rev. B 42 (1990) 6424.
[2] T. Ohzuku, Y. Iwakoshi, K. Sawai, J. Electrochem. Soc. 140 (1993) 2490.
[3] S.S. Zhang, K. Xu, T.R. Jow, J. Power Sources 160 (2006) 1349–1354.
[4] P.H.L. Notten, J.H.G. Op het Veld, J.R.G. van Beek, J. Power Sources 145 (2005) 89.
[5] P.C. Lin, Y.H. Liu, Y.H. Liu, J.K. Chen, C.H. Chen, Proceedings of 18th Symposium on Electrical Vehicles, Session D7A, 2001, pp. 1–13.
[6] Y.H. Liu, J.H. Teng, Y.C. Lin, IEEE Trans. Ind. Electron. 52 (2005) 1328.
[7] S.K. Chung, A.A. Andriiko, A.P. Mon'ko, S.H. Lee, J. Power Sources 79 (1999) 205.
[8] G. Sikha, P. Ramadass, B.S. Haran, R.E. White, B.N. Popov, J. Power Sources 122 (2003) 67.
[9] L.L. Lewyn, U.S. 5,670,862 (1997).
[10] Y.M. Podrazhansky, M.Y. Podrazhansky, M.B. Golod, U.S. 5,504,415 (1996).
[11] J.F. Freiman, S.K. McConkey, N.A. Mitchell, U.S. 5,726,554 (1998).
[12] N. Mitchell, U.S. 6,040, 684 (2000).
[13] J. Li, E. Murphy, J. Winnick, P.A. Kohl, J. Power Sources 102 (2001) 302.
[14] G. Nagasubramanian, J. Power Sources 87 (2000) 226.